Development of silicon detectors for Beam Loss Monitoring at HL-LHC

2017 JINST 12 C03036

(http://iopscience.iop.org/1748-0221/12/03/C03036)

Jinst

Published by IOP Publishing for Sissa Medialab

Received: *December 6, 2016*
Revised: *January 18, 2017*
Accepted: *February 23, 2017*
Published: *March 9, 2017*

14th Topical Seminar on Innovative Particle and Radiation Detectors
3–6 October 2016
Siena, Italy

Development of silicon detectors for Beam Loss Monitoring at HL-LHC

E. Verbitskaya,[a,1] **V. Eremin,**[a] **A. Zabrodskii,**[a] **A. Bogdanov,**[a] **A. Shepelev,**[a] **B. Dehning,**[b,2] **M.R. Bartosik,**[b,c] **A. Alexopoulos,**[b,d] **M. Glaser,**[b] **F. Ravotti,**[b] **M. Sapinski,**[e] **J. Härkönen,**[f] **N. Egorov**[g] **and A. Galkin**[h]

[a] *Division of Solid-State Electronics, Ioffe Institute, 26 Politekhnicheskaya, St. Petersburg 194021, Russian Federation*
[b] *CERN, CH-1211, Geneva 23, Switzerland*
[c] *Institute for Particle Physics, ETH Zurich, Otto-Stern-Weg 5, 8093 Zurich, Switzerland*
[d] *Department of Computer Science, University of Thessaly, Papasiopoulou 2-4, P.C. 35100-Galaneika, Lamia, Greece*
[e] *GSI Helmholtzzentrum für Schwerionenforschung, Planckstrasse 1, Darmstadt, D-64291 Germany*
[f] *Division of Experimental Physics, Ruđer Bošković Institute, Bijenička cesta 54, 10000, Zagreb, Croatia*
[g] *Research Institute of Material Science and Technology, 4 Passage 4806, Moscow, Zelenograd 124460, Russian Federation*
[h] *Centre of Technical Support "NAUKA", 126 prospect Mira, Moscow 129085, Russian Federation*

E-mail: elena.verbitskaya@cern.ch

Abstract: Silicon detectors were proposed as novel Beam Loss Monitors (BLM) for the control of the radiation environment in the vicinity of the superconductive magnets of the High-Luminosity Large Hadron Collider. The present work is aimed at enhancing the BLM sensitivity and therefore the capability of triggering the beam abort system before a critical radiation load hits the superconductive coils. We report here the results of three *in situ* irradiation tests of Si detectors carried out at the CERN PS at 1.9–4.2 K. The main experimental result is that all silicon detectors survived

[1] Corresponding author.
[2] Deceased on January 14, 2017.

doi:10.1088/1748-0221/12/03/C03036

irradiation up to 1.22×10^{16} p/cm^2. The third test, focused on the detailed characterization of the detectors with standard (300 μm) and reduced (100 μm) thicknesses, showed only a marginal difference in the sensitivity of thinned detectors in the entire fluence range and a smaller rate of signal degradation that promotes their use as BLMs. The irradiation campaigns produced new information on radiation damage and carrier transport in Si detectors irradiated at the temperatures of 1.9–4.2 K. The results were encouraging and permitted to initiate the production of the first BLM prototype modules which were installed at the end of the vessel containing the superconductive coil of a LHC magnet immersed in superfluid helium to be able to test the silicon detectors in real operational conditions.

KEYWORDS: Beam-line instrumentation (beam position and profile monitors; beam-intensity monitors; bunch length monitors); Cryogenic detectors; Radiation-hard detectors

2017 JINST 12 C03036

Contents

2017 JINST 12 C03036

1 Introduction

The outcome of particle physics experiments at the High-Luminosity Large Hadron Collider at CERN evidently depends on a reliable accelerator operation. In order to ensure this and prevent quench-provoking events in the superconducting magnets, installing beam loss monitors (BLMs) in the close vicinity of the magnet coils, i.e. inside superfluid helium (at a temperature T of 1.9 K), was found to be mandatory [1, 2].

The compactness of the novel BLM system can be realized by implementing semiconductor detectors. In particular, silicon detectors were considered to be used due to a well-developed technology of mass-production, high reproducibility of electrical characteristics of the devices delivered by commercial vendors, and cost-effectiveness. The challenge for their application as BLMs is radiation hardness in a harsh radiation environment at extremely low T inside the superconductive LHC magnets.

The properties of silicon as detector material and the radiation hardness of Si detectors have been widely investigated during the past decades, e.g. by different CERN R&D collaborations. The experimental studies, however, have been mostly limited to room-temperature (RT) operation or slightly cooled (down to −50°C) devices. Early investigations of silicon and Si detectors at low T can be divided into two categories.

1. Study of radiation damage introduced into the silicon raw material irradiated at $T = 4.2$ K [3]. The results showed that, among primary defects induced by radiation (electrons with the energy of 1–3 MeV), the interstitials became mobile at 4 K, whereas the vacancies started to be mobile at 70–200 K (depending on the silicon resistivity ρ).

2. Investigation of irradiated Si detectors while cooling from RT down to 130 K. The results showed a striking recovery of the charge collection efficiency, $CCE = Q_c/Q_o$ (where Q_c is the collected charge and Q_o the charge generated in the detector by impinging particles). This effect, known as the Lazarus effect, also led to the recovery of position resolution in Si microstrip detectors [4]–[6].

The results mentioned in point 1 led one to expect that the degradation of Si detectors by irradiation at 1.9 K would be largely inhibited because the formation of vacancy-related complexes, critical for radiation degradation, would be partially or even completely suppressed. On the other hand the measurements of the detectors characteristics at cryogenic T mentioned in point 2 were carried out with the samples irradiated at RT, which is not the case for BLM operation in the collider, and therefore could not give direct information on the detectors characteristics at T = 1.9–4.2 K.

The challenges arisen from the use of Si detectors as BLMs motivated the investigations of their radiation hardness at extremely low temperatures. The project entitled as "Si cryogenic BLMs" was carried out by the CERN-BE-BI-BL group and the CERN-RD39 collaboration ("Cryogenic Tracking Detectors") since 2011. In this report the results on the characterization of Si detectors intended to be operated as BLMs are presented. The characteristics are measured prior to irradiation at T = 4.2 K and in irradiation campaigns at T = 1.9–4.2 K. The overview of three *in situ* irradiation tests (T1–T3) is presented emphasizing the experimental results from our latest experiment carried out in 2015. The new findings in the physics of radiation damage and carrier transport in silicon p-n junction detectors at 1.9–4.2 K are described.

2 Experimental samples and measurement technique

In the investigations of Si detectors developed as BLMs the timeline and the sequence of the measurements at T = 1.9–4.2 K were the following.

- 2012: characterization of nonirradiated Si detectors at 4.2 K (the test denoted as T0) [7];
- 2012: the first *in situ* irradiation test (T1) aimed at getting the first data on detector radiation degradation at 1.9 K, and performed with detectors processed on wafers with a standard thickness (d) of 300 μm and different silicon resistivities [8, 9];
- 2014: the second *in situ* irradiation test (T2) aimed at the first comparison between the radiation degradations at T = 4.2 K of detectors with standard and reduced (100 μm) thicknesses [10];
- 2015: the third *in situ* irradiation test (T3) at T = 4.2 K focused at getting statistically significant data on the signal degradation in modules of Si detectors with 300 and 100 μm thicknesses.

The silicon samples used in all the tests were planar p^+-n-n^+ pad detectors designed and manufactured jointly by the Ioffe Institute, St. Petersburg, and the Research Institute of Material Science and Technology, Zelenograd, both Russia. The detectors were processed mainly on wafers with a resistivity of 10–15 kΩcm.

In situ irradiation tests were carried out at the CERN PS. The detectors were irradiated by a proton beam with an energy of 23 GeV and a beam diameter of about 1 cm at the detector position. The maximum fluence was in the range $2\times10^{15} - 1.22\times10^{16}$ p/cm^2. The beam intensity was around 1×10^{11} p/cm^2 in a spill with duration of 400–470 ms. Monitoring of the beam position and the intensity was performed along the entire duration of the tests by the Beam Position Monitors (BMP) incorporated in the PS facility. The detector modules were mounted in a cassette installed inside a

2017 JINST 12 C03036

cryostat with superfluid or liquid helium. In addition to BMPs two silicon beam telescope modules each containing four Si detectors were used to control alignment of the cassette with respect to the beam at the beginning of the irradiation.

The experimental study of the detectors included the following measurements:

- the I-V characteristics,
- the current pulse response of the detector arising from the nonequilibrium charge generated by a spill,
- the collected charge Q_c determined by integrating the current response over a spill duration (T2 and T3),
- the current pulse response using the Transient Current Technique (TCT) with an oscilloscope (3 GHz bandwidth) and a 680 nm laser with a pulse duration of about 45 ps illuminating the detector contacts; these measurements were performed in T0 and T1.

The measurements of the I-V characteristics and the dependences of the collected charge vs. bias voltage (V) and proton fluence (F) were carried out at reverse ($V_{\rm rev}$) and forward ($V_{\rm forw}$) bias voltages. The latter corresponds to the Current Injection Detectors (CID) suggested earlier for an effective charge collection in irradiated Si detectors operated at cryogenic T [11]. To implement this, the detectors have to be damaged by radiation so that the concentration of the defects with deep energy levels in the silicon bulk would be sufficient to stabilize the electric field distribution; this occurs at the equivalent neutron fluence of (1–5) $\times 10^{15}$ n_{eq}/cm^2. The detailed description of the cryogenic system utilized and of the measurements of the detectors characteristics is given in [7–9].

One of the objectives in T3 was a larger number of samples allowing to obtain statistically significant results on the detector signal. This is denoted as "statistics" in table 1 where the parameters of eight detectors modules including 26 detectors are listed.

Table 1. Parameters of detector modules studied in the test T3.

module	detector numbering in modules	ρ (kΩcm)	d (μm)	detector area (mm^2)	bias voltage (V)	purpose	readout
TeleIN	1–4	$\geqslant 15$	300	12×12	200	telescope "IN"	oscilloscope
MM1	1–4	$\geqslant 15$	300	5×5	400	statistics	Ioffe-DAQ
MM2	5–8	~ 0.5	300	5×5	500	statistics	Ioffe-DAQ
MM3	9–12	$\geqslant 15$	100	5×5	500	statistics	Ioffe-DAQ
MM4	13–16	$\geqslant 15$	100	5×5	400	statistics	Ioffe-DAQ
Ref1	1	$\geqslant 15$	300	5×5	400	test of DAQ system	CERN-DAQ
Ref2	1	$\geqslant 15$	300	5×5	400	test of DAQ system	CERN-DAQ
TeleOUT	1–4	$\geqslant 15$	300	12×12	200	telescope "OUT"	oscilloscope

Sixteen detectors dedicated to the statistical study were combined into the modules MM1–MM4, each involving four identical samples numbered sequentially from 1 to 16. A compact arrangement with a minimum gap between the detectors in the modules resulted in diminishing the fluctuations of the proton beam intensity and of the accumulated fluence. Two of the modules

labeled as "TeleIN" and "TeleOUT" also contained four samples each and were exploited as beam telescopes located near the entrance and exit planes of the cassette with installed modules. The reference detectors denoted as Ref1 and Ref2 were identical to those in the module MM1. These detectors were needed to compare the data recorded by different DAQ systems. Metallization of the front sample contact was continuous for all detectors except the detectors Ref1 and Ref2 where aluminum was mesh patterned. Figure 1a shows a schematic cross-section of the detector irradiation typical of tests T1–T3. The cassette with the installed detector modules studied in T3 is presented in figure 1b.

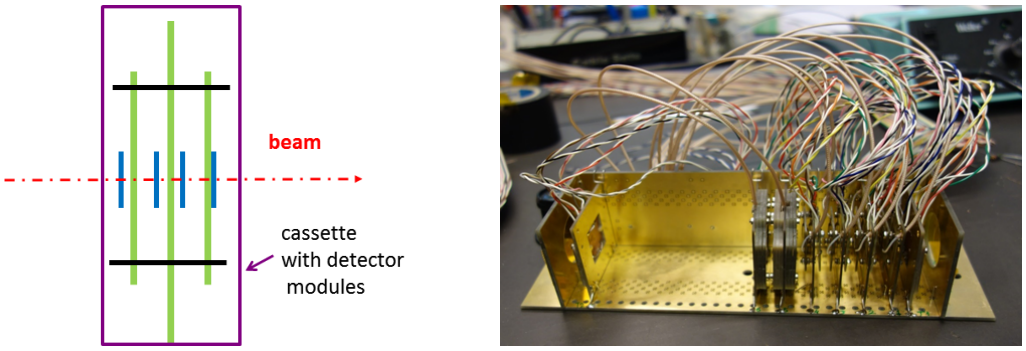

Figure 1. Schematic cross-section of the detector irradiation in the tests T1–T3 (a), and the cassette with the detector modules studied in the test T3.

The increased number of detectors studied in T3 required upgrading the cryostat units and the DAQ system. The cryostat upgrade consisted in the implementation of an output multichannel flange coupled with the DAQ systems and guide rails mounted on the inner cryostat wall. The latter allowed improving the cassette orientation with respect to the beam. Two versions of the DAQ system were used in T3. The first was the CERN-DAQ system coupled with the two reference detectors. The system automatically recorded the signals from each spill at a fixed bias voltage during the total period of the experiment (three weeks) and was stopped only when the $Q_c(V)$ dependences (so called voltage scans) were measured. The second was the DAQ system developed at the Ioffe Institute, which included a 16-channel sampling unit with an incorporated ADC operated at the sampling frequency of 250 Hz and linked with the detectors from the modules MM1–MM4. The signal from the individual detector was amplified, digitized in the nonstop regime, and, after being triggered, recorded by a PC. The trigger signal was generated externally by one of the telescope detectors and so was synchronized with the arrival time of the spill. This system recorded the signals automatically all over the T3 duration and manually whiles the voltage scans were carried out.

Monitoring of the beam parameters by BMPs showed that its intensity and position were not stable in time. Hence, the raw data were filtered to exclude the periods of abnormal values of the beam parameters. The filtered BPM data were employed to build a 3D image of the beam. By taking into account the geometry and the relative positions of the detectors, the number of protons delivered by the spill and passed through the detectors was obtained. This number was used to recalculate the detector signal recorded by the DAQ systems into the charge generated by a single proton (mip) and collected in the detector. The error of the signal measurements in T3 was about ±10%.

3 Overview of the results obtained in the tests T0-T2

The main result of the test T0 was "Proof of the concept" i.e. the demonstration of the proper operation of the p^+-n-n^+ silicon pad detectors in liquid helium via the measurements of the current pulse response and the definition of the carrier transport parameters [7]. It was carried out using TCT with the laser light illuminating the detector contacts. A surprising result was that the tops of the response shapes were not flat as it should be due to carrier freezing at shallow levels of dopants in silicon expected at 4 K. In this case the electric field profile should be uniform thus giving flat tops of the pulse shapes. However, descending and ascending slopes were observed in the shapes of the current pulses arisen from the electron and the hole drift (illumination of the p^+ and n^+ contacts, respectively), which were similar to the response shapes at *RT*. The results verified that the structure of the p^+-n-n^+ diode provided efficient charge collection at $T = 4.2$ K.

The test T1 was the longest (about six weeks) and involved the total set of measurements mentioned in section 2. The results showed that [8, 9]:

- all detectors survived with an appropriate *CCE* the irradiation up to 1.22×10 p/cm^2 and at this fluence the CCE was independent of the silicon resistivity;
- silicon detector operation in the CID mode was feasible and showed an advantage in the detector signal at $F < 5 \times 10^{15}$ p/cm^2 (mainly at lower bias voltages);
- the rate of the signal degradation was about seven times higher than that for *RT* irradiation;
- at $F \sim 5 \times 10^{13}$ p/cm^2 the current pulse response obtained in the TCT measurements had a double-peak shape, which was an indication of space charge sign inversion typical of prevailing introduction of vacancy-related acceptor-type radiation defects in contrast with the results expected from [3].

The test T2 was focused on the first comparison of the signals from irradiated Si detectors with standard and reduced thicknesses [10]. The use of thinned (100 μm) detectors as BLMs is stimulated by two factors. The first one is an extension of the operational fluence range, as shown in figure 2 by the dependence on fluence of the normalized charge collected in 100 and 300 μm thick detectors. These curves were calculated using the Hecht equation and the values of the carrier trapping time constants $\tau_{e,h}$ derived from the T1 data [9]. The second favorable factor is a higher mean electric field $\bar{E} = V/d$ in a detector operated at the same bias voltage V as a 300 μm thick detector. This is helpful in increasing the carrier drift velocity i.e. reducing the carrier collection time and trapping-related charge losses, and suppressing the possible effect of polarization. The advantages of thinned detectors are illustrated in figure 3 where the experimental $Q_c(V)$ dependences are compared for the detectors with 300 and 100 μm thicknesses irradiated to F around 1.5×10^{15} p/cm^2. Here and in figures 6 and 7 presented in section 4 $V_{\rm rev}$ and $V_{\rm forw}$ correspond to the negative and positive voltages, respectively, applied to the detector p^+ contact. The data in figure 3 showed that at the same bias voltage the charge collected in the 100 μm thick detector was higher than in the 300 μm thick one although the nonequilibrium charge Q_o generated by mips in a 300 μm thick detector was threefold larger than in a 100 μm thick one (24 and 8 ke, respectively). Operation of the detectors in the CID mode also gave a higher collected charge in the thinned detectors as it was observed at $F \leqslant 2 \times 10^{15}$ p/cm^2 and lower $V_{\rm forw}$.

2017 JINST 12 C03036

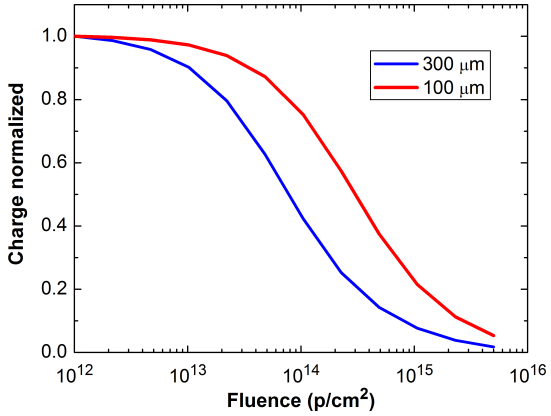

Figure 2. Calculated dependences of normalized collected charge on fluence for Si detectors with standard and reduced thicknesses. $T = 1.9$ K.

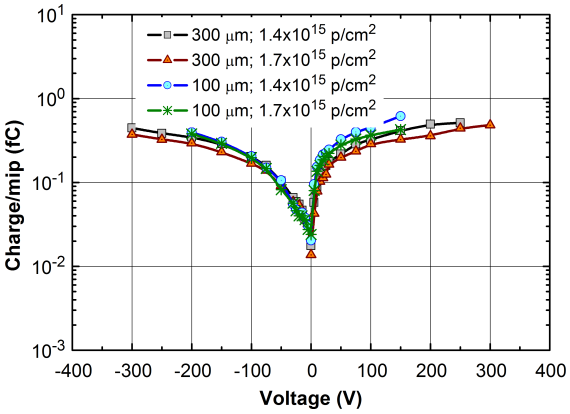

Figure 3. Experimental dependences on bias voltage of the charge collected in irradiated 300 and 100 μm thick detectors obtained in T2. Negative and positive voltages correspond to $V_{\rm rev}$ and $V_{\rm forw}$, respectively.

4 Results of the *in situ* irradiation test T3

The main goal of the test T3 was getting a statistically reliable verification of the results obtained in the tests T1 and T2. For this reason systematic measurements of the detector responses with beam spills while *in situ* irradiating up to 6×10^{15} p/cm^2, were carried out at different bias voltages including $V_{\rm forw}$. Unfortunately the initial data at zero and low F were missed due to technical faults.

As an example, figure 4 shows the current signals generated by a single spill in the detectors Ref1 (CH1) and Ref2 (CH3) irradiated to three different fluences in the range $(1.66–5.9) \times 10^{15}$ p/cm^2 and recorded by the CERN-DAQ system. It can be seen that at a fixed F the current response shapes of two detectors were exactly the same, whereas the changes of the shapes with the increasing fluence were quite substantial. At $F = 1.66 \times 10^{15}$ p/cm^2 a maximum signal amplitude was observed at the end of the response rising edge (about 15 ms). At higher fluences of 3.1×10^{15} and 5.9×10^{15} p/cm^2 the response shapes became blurred and it was hard to identify unambiguously the rise and the decay times, whereas the maximum current amplitude shifted sequentially towards the middle of the spill width. Fluctuations of the signal amplitude in time were also observed in the current responses for the detectors from the modules MM1-MM4 recorded by another DAQ system. The reasons of these variations arising with the fluence accumulation are not clear yet.

Another illustration of the signal reproducibility is presented in figure 5 where the signal vs. fluence dependences for all detectors installed in the modules MM1–MM4 (a–d, respectively) are shown at $V_{\rm rev} = -300$ V. Here and in figures 6 and 7a the signal is expressed as the charge collected per mip, which was determined by integrating the individual current responses from a single spill recorded by the Ioffe Institute DAQ system over the whole spill duration and averaging the values recorded for two spill cycles (8–10 spills randomly distributed in time). The corresponding number of protons passed through the detectors was calculated from the BMP data as described in section 2.

At a fixed V the signal spread in the 300 μm thick detectors (figure 5, a and b) was higher than that in the 100 μm thick ones. The maximum spread was observed for the samples from the module MM2 processed on the 500 Ωcm silicon. It indicated presumably the problems with the

2017 JINST 12 C03036

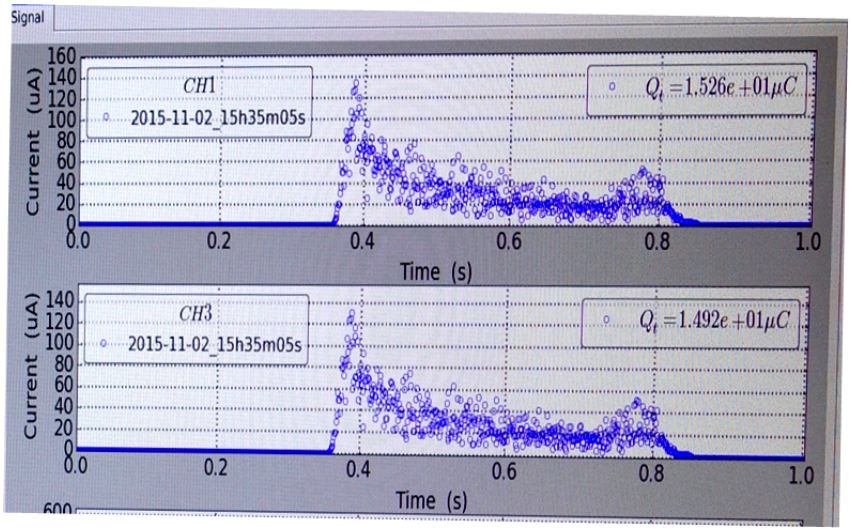

(a)

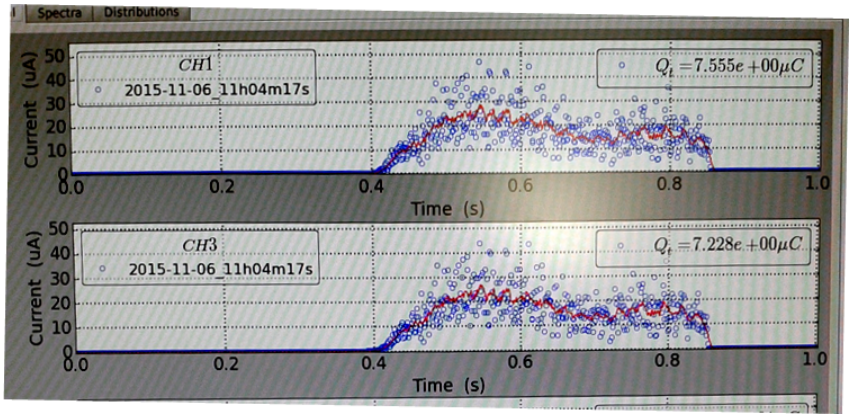

(b)

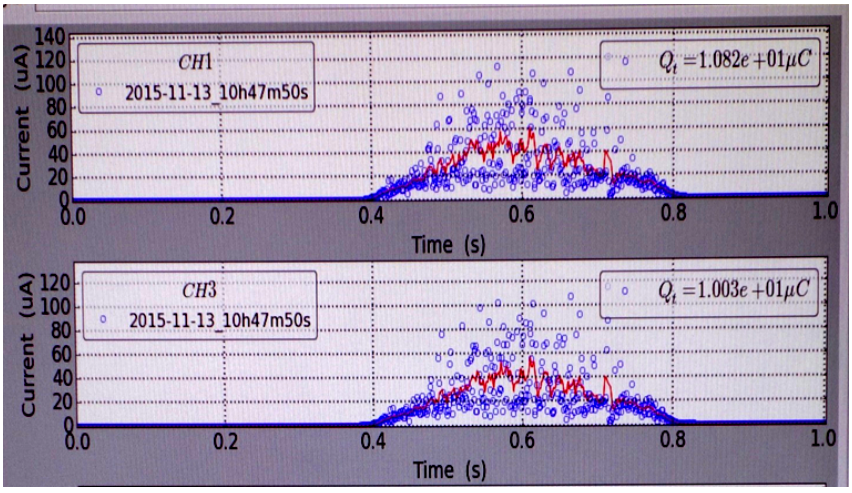

(c)

Figure 4. Current pulse signals arising from spills in irradiated detectors Ref1 (CH1) and Ref2 (CH3). F, 10^{15} p/cm^2: a — 1.66, b — 3.13, c — 5.9. $V_{\text{rev}} = -300$ V.

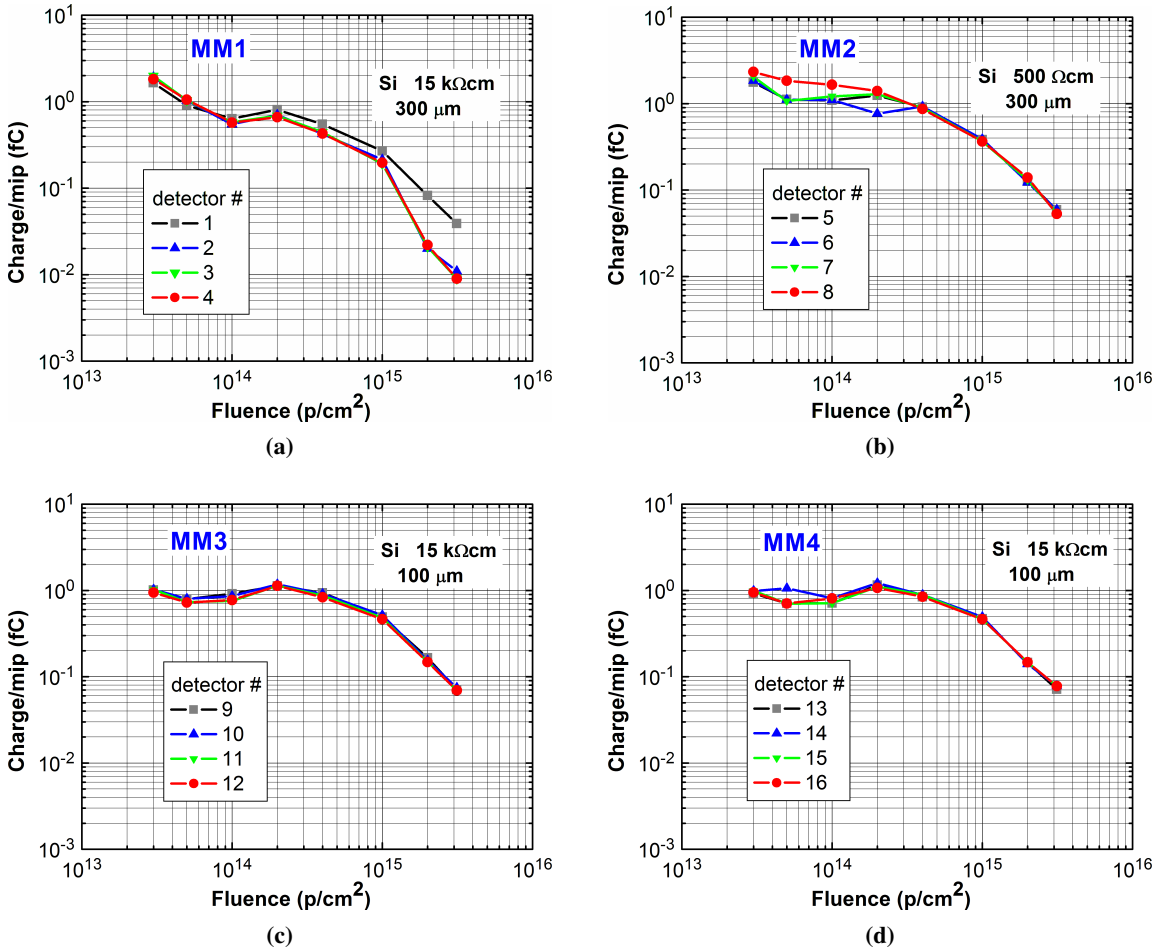

Figure 5. Dependences of the collected charge vs. fluence for the detectors from the modules MM1-MM4 (a-d, respectively) illustrating signal statistics. $V_{\rm rev} = -300$ V.

electric field distribution inside the bulk, which could be due to insufficiently optimized processing of the detectors made of this silicon grade. On the other hand, the signal spread was minimal in the 100 μm thick detectors (figure 5, c and d), especially in the module MM3. The specific feature of the curves shown in figure 5 is that for a majority of the detectors (13 from 16) signal reduction differed from the usual monotonic degradation with irradiation. The maximum signals of the detectors from MM3 and MM4 were shifted to $F = 2 \times 10^{14}$ p/cm^2 while for the six detectors from MM1 and MM2 only a marginal signal increase was observed at this fluence.

A similar shift was observed in the $Q_c(V)$ dependences for detectors irradiated within the fluence range $3.8 \times 10^{13} - 5.5 \times 10^{15}$ p/cm^2 and operated at $V_{\rm rev}$. These data are shown for the detectors MM1-1 and MM3-9 in figure 6, a and b, respectively. At $V_{\rm rev}$ and minimum F of 3.8×10^{13} p/cm^2 the curves showed saturation, which was evidence of full depletion of the 100 and 300 μm thick detectors. As seen in figure 6, above an irradiation fluence of 3.8×10^{13} p/cm^2 we did not observe saturation of collected charge at any forward or reverse bias voltage. The charge collected in the detector MM3-9 operated at $V_{\rm rev}$ and irradiated to 1.1×10^{14} and 5×10^{14} p/cm^2

2017 JINST 12 C03036

increased with the bias and at the absolute value of V_{rev} (absV_{rev}) above 150 V became larger than the corresponding charge in the detector irradiated to 3.8×10^{13} p/cm^2. This feature was less pronounced in the 300 μm thick detectors from the modules MM1 and MM2. To confirm this abnormal behavior, in figure 7a the $Q_c(V_{rev})$ data are presented for two 100 μm thick detectors from the module MM3 irradiated to 3.8×10^{13} p/cm^2 and the curves are clearly similar. However, at $F = 1 \times 10^{15}$ p/cm^2 this abnormal behavior vanished and the collected charge was lower than Q_c collected in the detectors irradiated to 1.1×10^{14} p/cm^2. At $F > 1 \times 10^{15}$ p/cm^2 the charges collected at V_{rev} and V_{forw} had close values in the detectors with both thicknesses although at lower V_{forw} a larger Q_c was still observed in the CID mode. This difference disappeared finally in the detectors irradiated to $F \geqslant 5 \times 10^{15}$ p/cm^2.

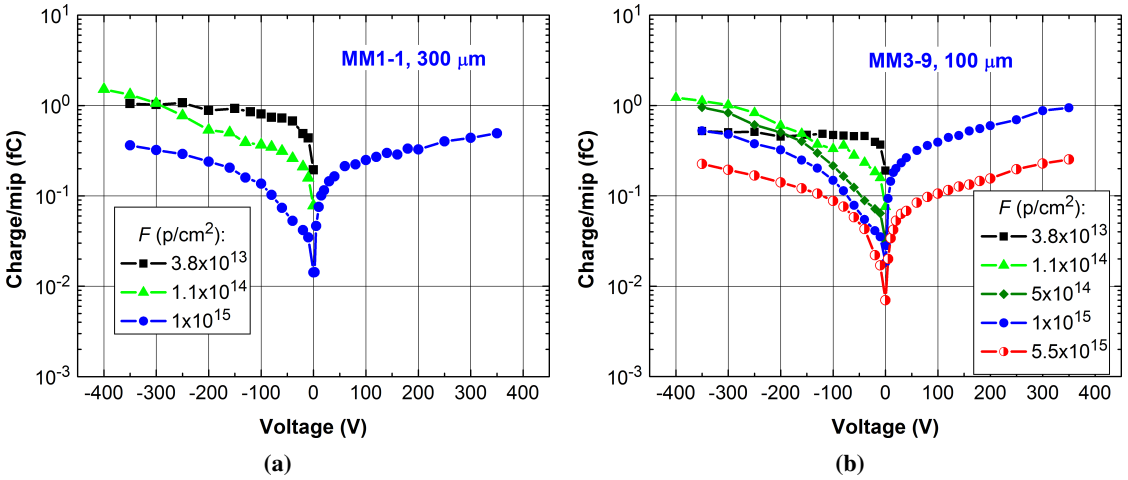

Figure 6. Dependences of the collected charge on the bias voltage in irradiated detectors with 300 (a) and 100 (b) μm thicknesses.

The advantage in terms of charge collected in thinner detectors can be seen in figure 7a where the voltage scan data are compared directly for 100 and 300 μm thick detectors. Finally, it becomes obvious from the values of the *CCE* (figure 7b). The values were calculated taking into account that the ratio of nonequilibrium charges generated by MIPs in the samples with 300 and 100 mm thicknesses, $Q_o(300)/Q_o(100)$, equals three. At the lowest F of $3.8{\times}10^{13}$ p/cm^2 and abs$V_{rev} \geqslant 150$ V $CCE(100)$ is about 50% higher than $CCE(300)$, whereas at $F = 1{\times}10^{15}$ p/cm^2 the ratio $CCE(100)/CCE(300)$ increases and reaches 3 and 5–6 at V_{rev} and V_{forw}, respectively. The higher efficiency of thinned detectors is due to two factors: 1) the mean electric field is higher than in the 300 μm thick ones, and 2) even at $F \sim 1 \times 10^{15}$ p/cm^2 the carrier drift length is comparable with the detector thickness, which leads to lower trapping-related charge losses. Finally, it results in a lower rate of radiation degradation in thinner detectors, which agrees with the calculated data shown in figure 2.

5 Summary

The results obtained in the study of silicon detectors developed as BLMs and characterized at 4.2 K before irradiation and in the *in situ* irradiation tests at 1.9–4.2 K can be divided into two groups.

2017 JINST 12 C03036

The first group includes clearly established results and some suggestions. Carrier saturation velocities and low-field mobilities in nonirradiated Si detectors at 4.2 K and the dependences of the trapping time constants on fluence at 1.9 K were defined. The rate of signal degradation in the 300 μm detectors at 1.9 K was shown to be seven times higher than that at *RT*. The changes of the current pulse shapes under irradiation suggested the introduction of vacancy-related acceptor-type defects, which was not expected.

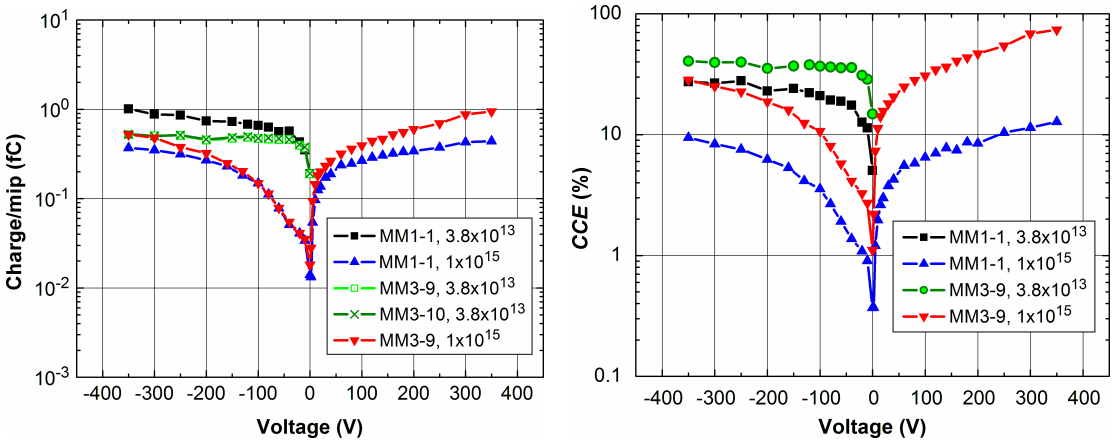

Figure 7. Comparison of the collected charges (a) and *CCE* (b) in irradiated detectors with 100 and 300 μm thicknesses.

The second group involves results relevant to detector operation as BLMs. It was shown that Si detectors can operate at 1.9 K after irradiation to $F = 1\times10^{16}$ p/cm^2 required for their application as BLMs. Operation in the CID mode was advantageous up to $F \sim 2\times10^{15}$ p/cm^2. Thinned (100 μm) detectors provided a significantly higher *CCE*, a lower rate of signal degradation, and minimum spread of the signal.

It should be noted that the explanations of some observations are not yet fully understood. The much larger signal degradation with fluence at cryogenic T compared to *RT* is related to a significant reduction of the carrier trapping time constants τ as defined via fitting the experimental $Q_c(F)$ dependences [9]. The other observation which requires further physical study is the double-peak shape of the current pulse response typical of prevailing introduction of acceptor-type defects. The reason of these effects can be related to the absence of self-annealing of unstable defects at 1.9–4.2 K, which usually takes place at *RT*. The development of physical models of Si detector operation at the temperatures of liquid and superfluid helium and further experimental studies are in progress.

As a consequence of our work silicon detector modules were installed on the end of the vessel containing superconductive coil of a magnet immersed in superfluid helium for their operation as BLMs in real experimental conditions [10, 12].

Acknowledgments

This work was supported in part by the Fundamental Program of the Russian Academy of Sciences "High Energy Physics and Neutrino Astrophysics." The preparation of this article was overshadowed

by the passing away of Dr. Bernd Dehning. Without his breakthrough ideas, broad knowledge and experience we would not have succeed. In sorrow we dedicate this article to his memory.

References

[1] C. Kurfürst et al., *Investigation of the use of silicon, diamond and liquid helium detectors for beam loss measurements at 2 K*, in *Proceedings of the IPAC2012*, New Orleans, U.S.A., May 20–25, 2012, p. 1080.

[2] O.R. Jones, *The beam instrumentation and diagnostic challenges for LHC operation at high energy*, in *Proceedings of the IBIC14*, Monterey, California, U.S.A., September 14–18, 2014, p. 216.

[3] G.D. Watkins, *EPR of Defects in Semiconductors: Past, Present, Future*, *Phys. Solid State* **41** (1999) 746.

[4] P. Rato Mendes, M.C. Abreu, S. Rodrigues, P. Sousa, V. Eremin, E. Verbitskaya et al., *A new technique for the investigation of deep levels on irradiated silicon based on the Lazarus effect*, *IEEE Trans. Nucl. Sci.* **51** (2004) 3069.

[5] P. Collins et al., *Cryogenic operation of silicon detectors*, *Nucl. Instrum. Meth.* **A 447** (2000) 151.

[6] RD39 collaboration, L. Casagrande et al., *Review on the development of cryogenic silicon detectors*, *Nucl. Instrum. Meth.* **A 461** (2001) 150.

[7] C. Kurfürst, *Cryogenic Beam Loss Monitoring at the LHC*, Ph.D. Thesis, Vienna TU, September 2013, Geneva.

[8] C. Kurfürst et al., *In situ radiation test of silicon and diamond detectors operating in superfluid helium and developed for beam loss monitoring*, *Nucl. Instrum. Meth.* **A 782** (2015) 149.

[9] E. Verbitskaya, V. Eremin, A. Zabrodskii, B. Dehning, C. Kurfürst, M. Sapinski et al., *Charge collection in Si detectors irradiated in situ at superfluid helium temperature*, *Nucl. Instrum. Meth.* **A 796** (2015) 118.

[10] Z. Li, V. Eremin, E. Verbitskaya, B. Dehning, M. Sapinski, M.R. Bartosik et al., *CERN-RD39 collaboration activities aimed at cryogenic silicon detector application in high-luminosity Large Hadron Collider*, *Nucl. Instrum. Meth.* **A 824** (2016) 476.

[11] V. Eremin, J. Harkonen, P. Luukka, Z. Li, E. Verbitskaya, S. Vayrynen et al., *The operation and performance of Current Injected Detector (CID)*, *Nucl. Instrum. Meth.* **A 581** (2007) 356.

[12] M.R. Bartosik et al., *Cryogenic Beam Loss Monitors for the superconducting magnets of the LHC*, in *Proceedings of the IBIC14*, Monterey, California, U.S.A., September 14–18, 2014, p. 471.

2017 JINST 12 C03036